J. Coat. Technol. Res.
DOI 10.1007/s11998-010-9243-8

Structures and properties of the polyester nonwovens coated with titanium dioxide by reactive sputtering

Yang Xu, Huifeng Wang, Qufu Wei, Huishan Liu, Bingyao Deng

Abstract Nanoscale titanium dioxide (TiO_2) films were deposited on the surface of polyester nonwovens by using direct current (DC) reactive magnetron sputtering. The effect of coating thickness on the surface structures and properties of TiO_2 coated fabrics was investigated by atomic force microscope (AFM), X-ray diffraction (XRD), energy dispersive X-ray analysis system (EDX), scanning electron microscope (SEM), and antistatic test in this article. The results indicated that the grain sizes of the sputtered clusters increased and the coating layer became more compact as film thickness was increased, but the crystal structure did not have any significant change. At the same time, the film mechanical properties and antistatic performance in general depended strongly on the film thickness which could lead to the optimum thickness for a particular application.

Keywords Magnetron sputtering, Titanium dioxide, Nonwoven fabric, Surface, Antistatic

Introduction

Titanium dioxide thin films have been intensively studied since Fujishima and Honda found the photocatalytic decomposition of water on titanium dioxide (TiO_2).[1] When TiO_2 is illuminated by ultraviolet (UV) light with higher energy than TiO_2 bandwidth, interband transition is induced and results in the generation of electron–hole pairs. Such excited electrons and holes could diffuse to TiO_2 surface and generate some radicals or ions, which can decompose some organic compounds absorbed on TiO_2 surface.[2] The commercial use of TiO_2 as photocatalyst is becoming widespread in the areas of water purification, air purification, and sterilization/disinfection. Further applications of self-cleaning, transparent and antistatic films of TiO_2 on some substrates are beginning to be explored.[3] Polymer fabrics are often used as the substrate to carry the active coatings. The combination of polymer materials with TiO_2 functional coatings offers a number of key advantages over alternative bulk materials, such as high strength-to-weight ratio, resistance to corrosion, mechanical flexibility, and relatively low cost.[4]

Physical vapor deposition (PVD) processes such as magnetron sputtering has been found to be one of the efficient techniques to prepare TiO_2 thin films on textile substrate, due to its better adhesion to substrates, environmentally friendly process, and low-temperature deposition.[5–7] The versatility of nanoscale TiO_2 and the ability of deposition technology would lead to new applications and open up considerable potential for further applications of textile fabrics. However, coatings with thickness down in the nanometer range are often associated with growth heterogeneities and high residual stresses generated during the deposition process. Moreover, the thin, brittle oxide coating and coating/substrate assembly must resist externally applied mechanical and hydrothermal loads during all the conversion processes usually encountered in the manufacture of the products, and during service.[8] Therefore, the analysis of the coating microstructure with different thickness and its influence on the reliability of the functional performance of the TiO_2 coated fabrics is essential.

In this study, nanoscale TiO_2 films were deposited on the surface of polyester (PET) nonwovens by using direct current (DC) reactive magnetron sputtering at room temperature. In order to correlate the effect of the thickness on the coating reliability, a set of three samples of 20, 60, and 100 nm was produced. Atomic

Y. Xu, H. Wang, Q. Wei (✉), H. Liu, B. Deng
Key Laboratory of Eco-Textiles, Ministry of Education, Jiangnan University, Wuxi, Jiangsu 214122, China
e-mail: qfwei@jiangnan.edu.cn

Published online: 18 February 2010

force microscopy (AFM), X-ray diffraction (XRD), energy dispersive X-ray analysis system (EDX), scanning electron microscope (SEM), and antistatic tests were employed to study and compare surface morphology, microstructure, chemical composition, interfacial structures, and the antistatic performance of the materials, respectively.

Experimental

Materials preparation

The substrate used in this study was spun-bonded polyester nonwovens with an area mass of 100 g/m^2. The samples cut from the PET nonwovens were first immersed into acetone solution for 30 min to remove the organic solvent and particles attached to the material. The cut samples were then rinsed with de-ionized water twice and dried at the temperature of 40°C in an oven after rinsing. The dried samples were further cut into a size of 6 × 6 cm for sputtering.

Sputter coating

Sputtering coatings of TiO_2 were performed onto the surface of PET nonwoven substrate at room temperature in a magnetron sputter coating system supplied by Shenyang Juzhi Co, LTD. A high-purity titanium (Ti) target (diameter: 50 mm; purity: 99.99%) was mounted on the cathode. The target was placed below the substrate at a distance of 60 mm and the sputtered particles were deposited onto the side of PET nonwoven facing the target. To avoid the deformation of the substrate and the diffusion movement of the sputtered particles caused by high temperature, water-cooling was applied to control the temperature of the substrate during the sputtering process. The sputter chamber was first pumped to a base pressure of 1.5×10^{-3} Pa prior to the introduction of high-purity argon gas (99.999%) as the bombardment gas and high-purity oxygen gas (99.999%) as the reacting gas. The argon and oxygen gas flows were set at 80 and 12 sccm, respectively. During the sputtering, the substrate holder was kept rotating at a speed of 100 rpm to ensure the uniform deposition on the surface of the PET substrate. Thickness of the coating was monitored using a coating thickness detector (FTM-V) fixed in the sputtering chamber. Coating was performed at a pressure of 0.5 Pa with a power of 70 W. Coating thicknesses were 20, 60, and 100 nm, respectively.

Surface characterization

AFM observation

A Benyuan CSPM3300 Atomic Force Microscope (Guangzhou, China) was employed to examine the morphology and distribution of nanoscale TiO_2 on the fabric surfaces. Scanning was carried out in contact mode AFM with a silicon cantilever. All images were obtained at ambient conditions and images were analyzed by the Imager 4.40 Software equipped with CSPM3300 AFM.

XRD analysis

The crystal structure of TiO_2 thin films was characterized by X-ray diffraction (X Pert MPD PRO, Holland) with 2θ angle in the range of 10–60° using a Cu Kα radiation.

SEM and EDX

A SEM instrument (S-4800, HITACHI, Japan) was used to observe the interfacial structure between the substrate and TiO_2 coating. The influence of coating thickness on the cohesion and adhesion of the brittle oxide coating on the soft PET substrate was analyzed by the SEM images. In order to prevent charge build-up during SEM observations, the samples were coated with platinum.

The EDX unit connected to the SEM microscope was used to determine the chemical contents of elements presented in the surface of coated fabrics at an accelerating voltage of 20 kV.

Antistatic properties

The process and main parameters of antistatic tests were set according to the national standard FZ/T01042-1996 (the tests of static properties and half-dissipation time for textile materials) and GB/92-T12703-91 (the electrostatic test methods for textile). Antistatic properties of TiO_2 coated fabrics were measured with YG (B) 342D type fabric induced static tester (Da-rong Textile Instrument, Wenzhou, China). The samples were conditioned at 20 ± 2°C and 42 ± 2% RH (relative humidity) for 5 h. The sample size was 60 × 60 mm and they were fixed in a stainless steel device holder and charged for 30 s in 10 kV electric field using corona discharge plasma. The state half-dissipation time was measured and compared.

Results and discussion

Comparison in surface morphology

The AFM image reveals the morphology of the PET fiber surface of the uncoated nonwoven, as presented in Fig. 1a. It clearly shows that the uncoated PET fiber has a relatively smooth surface with some microdefects such as microcracks and point defects on it. The

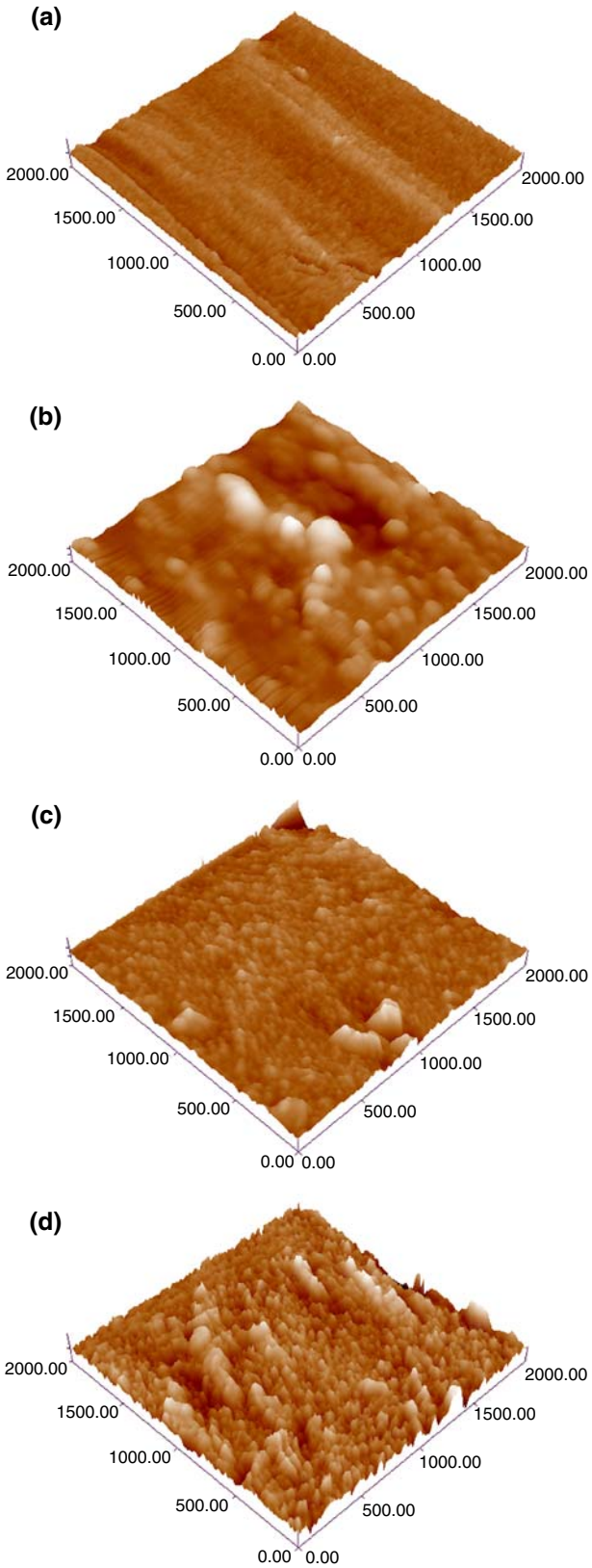

Fig. 1: AFM images of uncoated and coated PET fiber surface at the scan size of 2000 × 2000 nm: (a) uncoated, (b) 20 nm, (c) 60 nm, and (d) 100 nm

surface of the uncoated fiber shows clear periodic stripes which are probably formed during the fiber manufacturing process. The sputter coatings of TiO_2 significantly alter the surface characteristics of the PET fibers, as revealed in Figs. 1b–1d. The TiO_2 clusters scatter on the PET fiber surface after the 20 nm coating, but the clusters have variable sizes from less than 20 nm to over 50 nm, as illustrated in Fig. 1b. The intrinsic defects on PET surface may be responsible for the rough and loose structure of coating surface because the sputtering particles are preferential nucleation and growth at the defect location of substrate surface in the initial film growth stage.[9] As the coating thickness is increased to 60 nm, the TiO_2 clusters coated on the PET fiber surface have coalesced and look more even, the average size of the sputtered TiO_2 cluster is about 31.5 nm, an uninterrupted and compact coating is formed, as revealed in Fig. 1c. The AFM image in Fig. 1d indicates that the increased coating thickness from 60 nm to 100 nm leads to more compact distribution of the TiO_2 clusters on the fiber surface. The growth of the TiO_2 clusters is also observed and the size of the sputtered TiO_2 cluster is increased to 35.1 nm. This is attributed to the collision of the sputtered TiO_2 grains. The increase in sputter coating thickness leads to the growth of the TiO_2 clusters and more compact deposition.

XRD analyses

The XRD patterns of TiO_2 films deposited at different coating thickness look similar as shown in Fig. 2. It can be seen that all the samples only have PET characteristic peaks (2θ = 17.7°, 22.8°, and 25.7°) and have no diffraction peaks for crystalline TiO_2, which reveals the amorphous structure of the deposited TiO_2 films on the PET fibers. Anatase or rutile structure is not observed from the XRD analysis. This can be attributed to the TiO_2 deposition at room temperature. The thermal energy at the substrate is attained solely by the

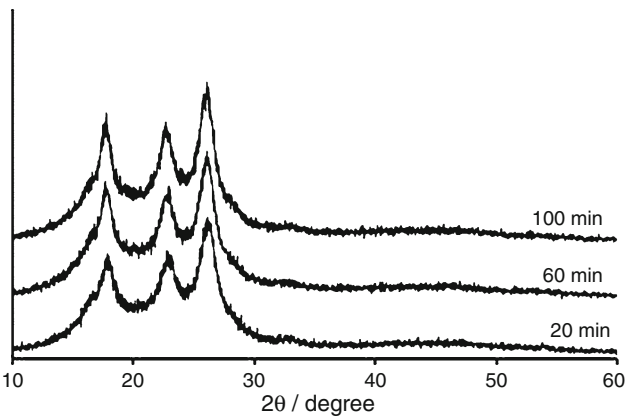

Fig. 2: XRD patterns of TiO_2 thin films deposited at different coating thickness of 20, 60, and 100 nm

deposition and ion bombardment fluxes. Consequently, a predominantly amorphous structure is obtained in the as-deposited state. It seems that the increase in coating thickness does not have any significant influence on the grain structure of the sputtered TiO_2 on the PET nonwoven surface.

EDX analysis

The functionalization of the PET nonwoven surfaces by sputter coatings of TiO_2 is also confirmed by EDX analyses. The EDX spectra in Fig. 3 show the PET nonwoven material before and after the TiO_2 sputter coatings. The atomic content percentages of elements are shown in Table 1. It can be seen in Fig. 3a that the surface of the nonwoven material dominantly consists of C and O before the sputter coating. The composition of hydrogen (H) in the material is too light to be detected in the EDX analysis.[10] Two clear peaks of Ti in the EDX spectrum after the TiO_2 coatings of 20, 60, and 100 nm can be seen in Figs. 3b, 3c, and 3d, respectively. The EDX peak intensity ratio at 4.5 keV may come from Ti K alpha and the 4.9 keV from Ti K beta. Compared with the EDX spectra of coating samples, the compositions of Ti and O are obviously increased and C is significantly reduced with the increasing thickness of coating. According to the analysis of the atomic content percentages of elements in Table 1, the increased amount of O and Ti reveals the presence of TiO_2 on the surface of the PET fiber after the reactive sputter coating of titanium in the mixed atmosphere of argon and oxygen.

SEM observations

After cutting the coated substrate as shown in Fig. 4, SEM was then used to observe the integrality of TiO_2 films around the cutting section and the interfacial bonding structure between TiO_2 thin films and substrates. As Fig. 5a shows, the deposited TiO_2 film of 20 nm around fiber looks fine without any cracking. Although the film is affected by cutting-force, the total cutting incision is clear and the interfacial bonding structure between coating and substrate on the edge of cutting incision looks good. The film of 60 nm is also uniform and fine, but a small part of the film on the

Table 1: Atomic content percentage of elements at different TiO_2 coating thickness

Coating thickness	Uncoated	20 nm	60 nm	100 nm
C (%)	76.14	56.76	39.04	23.59
O (%)	23.86	39.87	46.25	58.83
Ti (%)	–	3.37	14.71	17.58

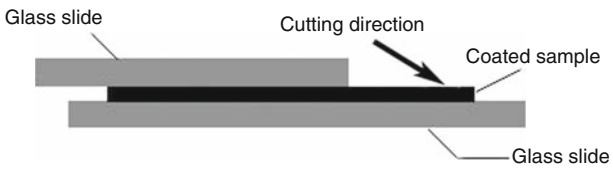

Fig. 4: Sectional view

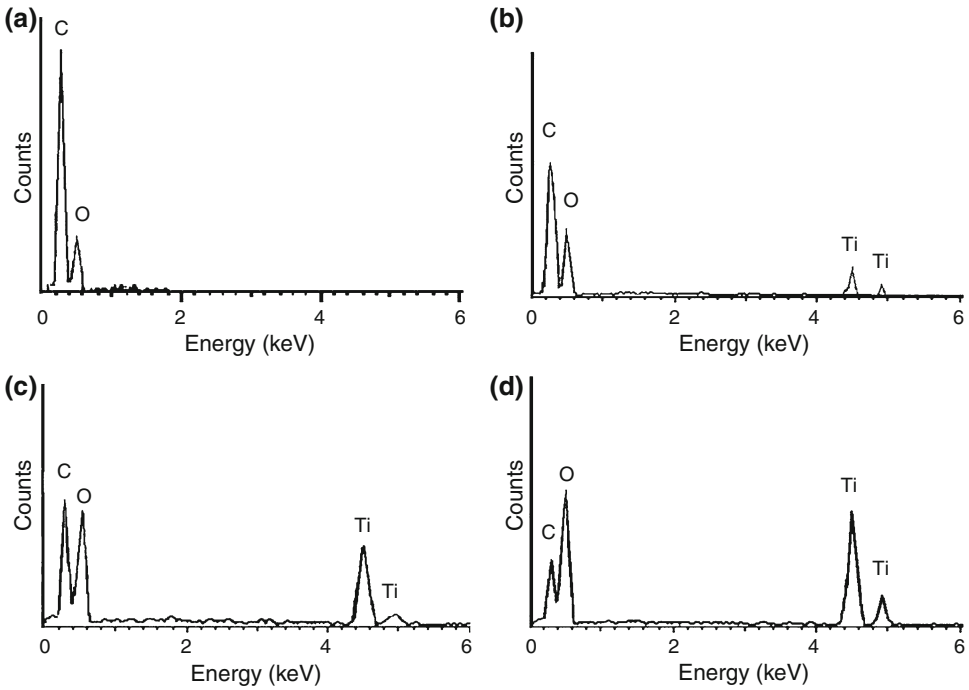

Fig. 3: EDX spectra of uncoated and coated PET nonwoven surface: (a) uncoated, (b) 20 nm, (c) 60 nm, and (d) 100 nm

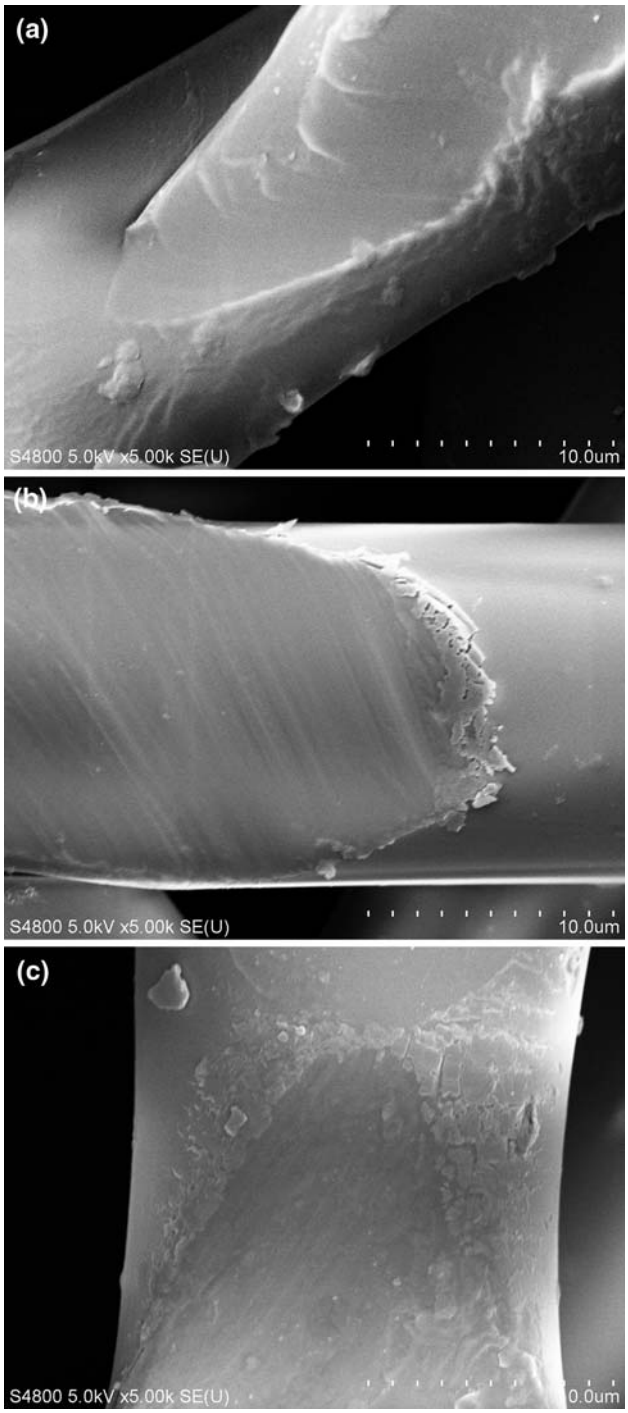

Fig. 5: SEM images of interface: (a) 20 nm, (b) 60 nm, and (c) 100 nm

edge of cutting incision area appeared to be cracked, as shown in Fig. 5b. As the coating thickness is increased to 100 nm, as shown in Fig. 5c, the film around the cutting section forms cracks and breaks up into some fragments by the cutting-force, and the interfacial structure between coating and substrate on the edge of cutting incision is associated with damage in the form

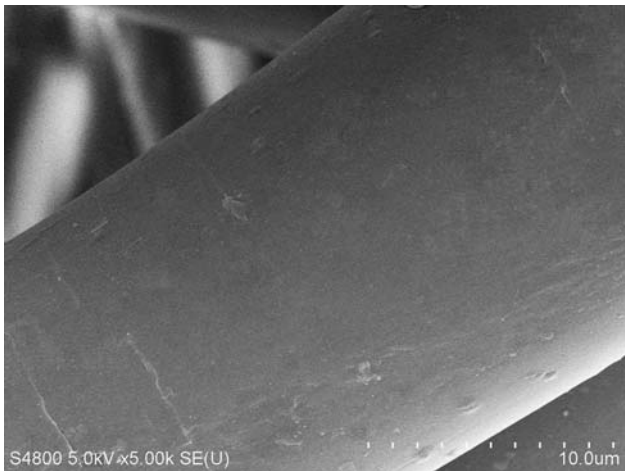

Fig. 6: Microcracks on the surface of 100 nm film

of loss of adhesion between the TiO_2 coating and PET fiber.

The thicker TiO_2 film cracked drastically after the cutting test may be due to the higher internal stress built up in the process. Internal stress is inherent to most multimaterial assemblies, where dissimilar materials with different thermo-mechanical properties are processed together. This also cannot be avoided in a combination of a PVD process with a low substrate temperature and highly refractory coating materials.[11] Further, after the sputtered cluster coalescence and an uninterrupted coating formed, the thicker the coating, the more compact structure and the higher growth stress is.[12] As a result of higher internal residual stress in thicker coatings, the film reliability is decreased. Because it may induce micron cracks on the surface of film leading to relaxation of deposition-induced internal stresses, as shown in Fig 6.

Antistatic properties

The half-dissipation time is used to evaluate the antistatic performance of the samples. It is the amount of time needed to reach half of the initial charge imposed by the test machine completely. It is one of more practical information for the antistatic performance. The shorter the half-dissipation time is, the better the antistatic ability of the fibers should be. Commercially available good antistatic material generally shows less than 3 s of the half-dissipation time.[13]

The test result of each sample is the average of three measurements, shown in Fig. 7. The half-dissipation time of uncoated fabrics is 37.3 s. This higher value is due to the inert nature of PET materials. Significant decrease in the half-dissipation time is observed for the 20 nm coated fabric as compared to uncoated fabric. The time for the surface charge to reach half of the initial surface charge is 11.8 s. As the coating thickness is increased to 60 nm, the half-dissipation time drops to 1.7 s, indicating excellent antistatic properties. After

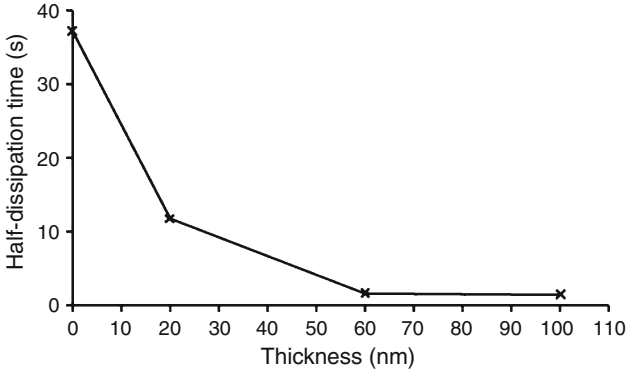

Fig. 7: The half-dissipation time of uncoated and coated PET nonwoven

which, it decreases slowly to 1.5 s when the coating thickness is increased to 100 nm. It may be due to the influence of more microcracks on the surface of thicker coatings, which block the discharge of surface assembled static charges.

Conclusions

This study has compared the effect of film thickness on growth and microstructure, chemical composition, and antistatic performance of TiO_2 coatings deposited by direct current magnetron sputtering at room temperature. The sputter coatings formed nanosized clusters scattered or covered on the fiber surface subject to the film thickness. Film thickness affected the grain sizes of the TiO_2 clusters. As the film thickness was increased, the grain sizes of the sputtered clusters increased and the coating layer became more compact, but the crystal structure did not have any significant change. The SEM analysis on cutting section structure indicated that thicker coatings were more prone to failure than thinner ones under the outside force due to the increased internal stress. By contrast, the antistatic performance of coated fabrics increased with increasing coating thickness.

Acknowledgment This work was supported by the Program for New Century Excellent Talents in University (NCET-06-0485) and Natural Science Foundation of Jiangsu Province (BK2008106).

References

1. Fujishima, A, Honda, K, ''Electrochemical Photolysis of Water at a Semiconductor Electrode.'' *Nature*, **5358** 37–38 (1972)
2. Liu, BS, Zhao, XJ, Zhao, QN, Li, CL, He, X, ''The Effect of O_2 Partial Pressure on the Structure and Photocatalytic Property of TiO_2 Films Prepared by Sputtering.'' *Mater. Chem. Phys.*, **90** 207–212 (2005)
3. Bozzi, A, Yuranova, T, Guasaquillo, I, Laub, D, Kiwi, J, ''Self-Cleaning of Modified Cotton Textiles by TiO_2 at Low Temperatures Under Daylight Irradiation.'' *J. Photochem. Photobiol. A: Chem.*, **174** 156–164 (2005)
4. Chen, Z, Cotterell, B, Wang, W, Guenther, E, Chua, SJ, ''A Mechanical Assessment of Flexible Optoelectronic Devices.'' *Thin Solid Films*, **394** 202–206 (2001)
5. Heo, CH, Lee, SB, Boo, JH, ''Deposition of TiO_2 Thin Films Using RF Magnetron Sputtering Method and Study of Their Surface Characteristics.'' *Thin Solid Films*, **475** 183–188 (2005)
6. Meille, V, ''Review on Methods to Deposit Catalysts on Structured Surfaces.'' *Appl. Catal. A: General*, **315** 1–17 (2006)
7. Boukrouh, S, Bensaha, R, Bourgeois, S, Finot, E, Marco de Lucas, MS, ''Reactive Direct Current Magnetron Sputtered TiO_2 Thin Films with Amorphous to Crystalline Structures.'' *Thin Solid Films*, **516** 6353–6358 (2008)
8. Leterrier, Y, ''Durability of Nanosized Oxygen-Barrier Coatings on Polymers.'' *Prog. Mater. Sci.*, **48** 1–55 (2003)
9. Liu, ZW, Gu, JF, Sun, CW, Zhang, QY, ''Study on Nucleation and Dynamic Scaling of Morphological Evolution of ZnO Film Deposition by Reactive Magnetron Sputtering.'' *Acta Phys. Sin.*, **55** 1965–1972 (2006)
10. Wei, QF, Yu, LY, Hou, DY, Wang, YY, ''Comparative Studies of Functional Nanostructures Sputtered on Polypropylene Nonwovens.'' *e-Polymers*, **039** 1–9 (2007)
11. Kusano, E, Kitagawa, M, Kuroda, Y, Nanto, H, Kinbara, A, ''Adhesion and Hardness of Compositionally Gradient TiO_2/Ti/TiN, ZrO_2/Zr/ZrN, and TiO_2/Ti/Zr/ZrN Coatings.'' *Thin Solid Films*, **334** 151–155 (1998)
12. Oberhauser, P, Abermann, R, ''Influence of Substrate Properties on the Growth of Titanium Films: Part IV.'' *Thin Solid Films*, **434** 24–29 (2003)
13. Kobayashi, T, Wood, BA, Takemura, A, Ono, H, ''Antistatic Performance and Morphological Observation of Ternary Blends of Poly(Ethylene Terephthalate), Poly(Ether Esteramide), and Na-neutralized Poly(Ethylene-co-Methacrylic Acid) Copolymers.'' *J. Electrostat.*, **64** 377–385 (2006)